CrossMark
click for updates

Glycolytic Dependency of High-Level Nitric Oxide Resistance and Virulence in *Staphylococcus aureus*

Nicholas P. Vitko, Nicole A. Spahich, Anthony R. Richardson

Department of Microbiology and Immunology, University of North Carolina at Chapel Hill, School of Medicine, Chapel Hill, North Carolina, USA

ABSTRACT *Staphylococcus aureus* is a prolific human pathogen capable of causing severe invasive disease with a myriad of presentations. The ability of *S. aureus* to cause infection is strongly linked with its capacity to overcome the effects of innate immunity, whether by directly killing immune cells or expressing factors that diminish the impact of immune effectors. One such scenario is the induction of lactic acid fermentation by *S. aureus* in response to host nitric oxide (NO·). This fermentative activity allows *S. aureus* to balance redox during NO·-induced respiration inhibition. However, little is known about the metabolic substrates and pathways that support this activity. Here, we identify glycolytic hexose catabolism as being essential for *S. aureus* growth in the presence of high levels of NO·. We determine that glycolysis supports *S. aureus* NO· resistance by allowing for ATP and precursor metabolite production in a redox-balanced and respiration-independent manner. We further demonstrate that glycolysis is required for NO· resistance during phagocytosis and that increased levels of extracellular glucose limit the effectiveness of phagocytic killing by enhancing NO· resistance. Finally, we demonstrate that *S. aureus* glycolysis is essential for virulence in both sepsis and skin/soft tissue models of infection in a time frame consistent with the induction of innate immunity and host NO· production.

IMPORTANCE *Staphylococcus aureus* is a leading human bacterial pathogen capable of causing a wide variety of diseases that, as a result of antibiotic resistance, are very difficult to treat. The frequency of *S. aureus* tissue invasion suggests that this bacterium has evolved to resist innate immunity and grow using the nutrients present in otherwise sterile host tissue. We have identified glycolysis as an essential component of *S. aureus* virulence and attribute its importance to promoting nitric oxide resistance and growth under low oxygen conditions. Our data suggest that diabetics, a patient population characterized by excess serum glucose, may be more susceptible to *S. aureus* as a result of increased glucose availability. Furthermore, the essential nature of *S. aureus* glycolysis indicates that a newly developed glycolysis inhibitor may be a highly effective treatment for *S. aureus* infections.

Address correspondence to Anthony R. Richardson, anthony_richardson@med.unc.edu.

*S*taphylococcus aureus is a Gram-positive bacterium capable of causing a wide variety of clinical manifestations in humans, including skin and soft tissue infections (SSTIs), pneumonia, bacteremia, endocarditis, and osteomyelitis. *S. aureus* infections are more common, invasive, and severe than those caused by coagulase-negative staphylococci (CNS), despite the shared colonization of human skin and frequent resistance to antibiotics (1, 2). The traditional explanation for this difference has been the acquisition of many unique virulence factors by *S. aureus* that promote colonization of fresh wounds and destruction of host tissues (3). Complementary to this concept is the hypothesis that an increased incidence of tissue invasion by *S. aureus* has led to metabolic adaptation that further distinguishes *S. aureus* from CNS. One instance where this is particularly evident is for the growth of *S. aureus* in the presence of the innate immune radical nitric oxide (NO·).

NO· is a small, membrane-permeable gas produced by activated phagocytes via an inducible nitric oxide synthase (iNOS or NOS2) (4). In this context, NO· acts as a broad-spectrum antimi-

crobial agent with a strong propensity for disrupting microbial metabolism, DNA replication, and lipid integrity (5). The effects of NO· are caused by direct binding of NO· to transition metals and/or organic radicals and indirectly via the formation of reactive nitrogen species (RNS), which themselves bind thiols, amines, and hydroxyl aromatic groups (6). Due to the high concentration of iron and thiol-containing enzymes in bacterial respiratory chains, a primary effect of NO· at levels of $\geq$500 nM is the disruption of cellular respiration (7, 8). In the context of infection, activated phagocytes can generate $\geq$1 μM NO· intracellularly (9, 10). While *S. aureus* strains can enzymatically detoxify NO· using the flavohemoprotein Hmp, mutants lacking this enzyme are still capable of replicating during nitrosative stress (11). Furthermore, despite possessing Hmp, CNS are incapable of growing in the presence of high levels of NO· (levels sufficient to inhibit cellular respiration) (8). Instead, what distinguishes *S. aureus* from CNS during growth under high levels of NO· is lactic acid fermentation.

Fermentation promotes *S. aureus* NO·-resistant growth by converting NADH into NAD$^+$ (i.e., balancing redox), which al-

lows for continued carbon catabolism via NAD^+-dependent pathways. During NO· exposure, *S. aureus* performs heterolactic acid fermentation using three lactic acid dehydrogenases (Ldh1, Ldh2, and Ddh) (8). Interestingly, CNS lack the *ldh1* allele and do not ferment lactate in response to NO· stress, despite possessing anaerobically responsive *ddh* and *ldh2* alleles (8). The reason for this discrepancy is currently unknown. However, we have demonstrated that NO·-dependent induction of *ldh1* in *S. aureus* is glucose dependent, leading us to consider the possibility that *S. aureus* growth in the presence of high NO· may itself be carbon source dependent (12).

Given the large contribution of NO· resistance to *S. aureus* infection and the metabolic basis for this unique resistance, we undertook a more extensive examination of the substrates that support *S. aureus* resistance to high levels of NO· (13). Our results indicate that *S. aureus* requires specific glycolytic substrates to grow in the presence of high levels of NO· *in vitro* and during phagocytosis. Furthermore, we demonstrate that glycolysis, but not gluconeogenesis, is required for *S. aureus* pathogenesis during murine infection. Together these results clearly establish the metabolic programming required for *S. aureus* to establish invasive infection, and in agreement with clinical observations, implicate the host glycemic state as an important factor in determining susceptibility to this pathogen.

RESULTS

Fermentative growth of *S. aureus* during NO· stress is glycolysis dependent. Unlike other pathogenic bacteria, including closely related staphylococci, *S. aureus* is capable of growing in the presence of high levels of nitric oxide (0.2 to 1 mM NO·) (8, 11). The identification of *ldh1* as a unique *S. aureus* NO· resistance factor implicates metabolic adaptation, specifically the induction of fermentative metabolism, as an important feature of high-level NO· resistance. However, little is known about the metabolic substrates and central metabolic pathways that support this resistance. Therefore, we examined the abilities of 10 different carbon sources (carbon balanced) to support growth of *S. aureus* under high NO· stress. High NO· stress was achieved using a mixture of NO· donors (1 mM diethylamine nitric oxide [DEANO] and 10 mM NOC-12), which achieve maximum [NO·] = ~1 mM by 1.5 h and maintain levels ≥500 nM for ~5 h. The carbon sources are loosely divided into two groups: glycolytic (glucose, sorbitol, mannose, and mannitol) and nonglycolytic (glycerol, gluconate, ribose, pyruvate, L-lactate, and Casamino Acids) (see Fig. S1 in the supplemental material). Only a subset of glycolytic carbon sources (hexoses) supported the growth of *S. aureus* in the presence of high NO· concentrations, while all of the nonglycolytic carbon sources failed to support growth (Fig. 1A and B). These phenotypes were confirmed using two additional *S. aureus* strains (Newman and SF8300) (data not shown).

Given the glycolytic dependency of *S. aureus* NO· resistance, we examined the contribution of the glycolysis-responsive regulator CcpA to growth under high nitrosative stress. However, there was no significant difference in the normalized maximum growth rates of wild-type and *ccpA*::Sp^r *S. aureus* during high nitrosative stress (47.1% ± 5.5% and 51.9% ± 5.4%, respectively). These data suggest that the dependency on hexoses for NO· resistance does not stem from CcpA-mediated induction of an unknown NO· resistance factor.

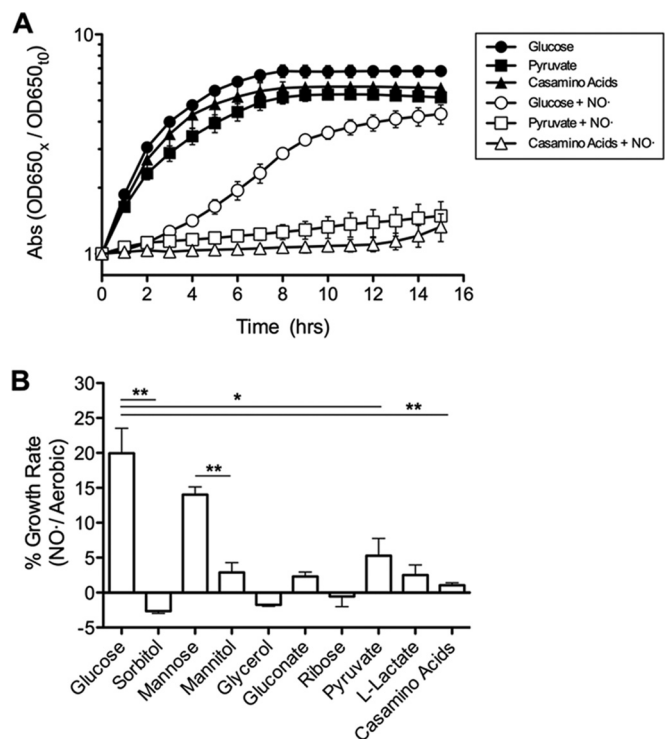**FIG 1** NO·-resistant growth of *S. aureus* is hexose dependent. (A) *S. aureus* COL grown at 37°C in CDM alone or with NO· mix with glucose (25 mM), pyruvate (50 mM), or Casamino Acids (0.5%) as the primary carbon source (*n* = 3; error bars show the standard errors of the means [SEM]). NO· mix was added at mid-log phase, and absorbance was normalized to the time of NO· addition (t0) (*n* = 3; error bars show SEM). Time (in hours) is shown on the *x* axis. (B) Average growth rates of *S. aureus* COL in CDM plus various primary carbon sources (carbon balanced to 25 mM glucose) following NO· exposure (NO· mix), normalized to the average mid-log aerobic growth rate in each carbon source (*n* = 3; error bars show SEM). Significance was calculated using a Student's two-sided *t* test (*, $P \leq 0.05$; **, $P \leq 0.01$).

Respiration inhibition partially explains the glycolysis dependence of *S. aureus* NO· resistance. The primary effect of high NO· levels is the inhibition of cellular respiration. Thus, we postulated that anaerobic growth of *S. aureus* would also be glycolysis dependent. Consistent with this hypothesis, growth of *S. aureus* during anaerobiosis was restricted to the same set of carbon sources that support NO· resistance, with one exception, pyruvate (Fig. 2A). Addition of the alternative electron acceptor nitrate (50 mM) to the media improved the anaerobic growth of *S. aureus* on all carbon sources. These anaerobic growth phenotypes were confirmed in two additional *S. aureus* strains (Newman and SF8300 [data not shown]). Furthermore, the respiration-deficient *S. aureus* menD::Er^r mutant, which lacks the ability to synthesize menaquinone electron carriers, exhibited the same carbon source-dependent growth under aerobic conditions as wild-type *S. aureus* grown anaerobically (e.g., glucose and pyruvate supported growth, but amino acids did not) (Fig. 2B). These data are consistent with NO·-dependent respiration inhibition as the primary cause of the observed carbon source constraints for *S. aureus* NO·-resistant growth, albeit not for pyruvate.

Fermentative growth of *S. aureus* on pyruvate requires acetogenesis. The observation that *S. aureus* growth on pyruvate is respiration independent suggests that NO· may directly inhibit
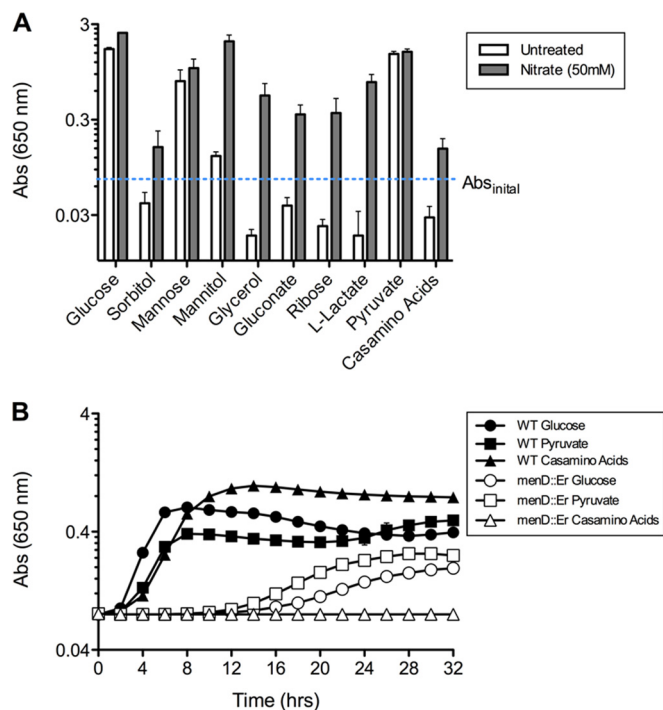
FIG 2 *S. aureus* growth on most carbon sources is respiration dependent. (A) Maximum absorbance (650 nm) of *S. aureus* COL grown at 37°C for 24 h anaerobically in CDM alone or with potassium nitrate (50 mM) with various primary carbon sources (carbon balanced to 25 mM glucose) (*n* = 3; error bars show SEM). (B) Aerobic growth of wild-type (WT) *S. aureus* Newman and *menD*::Er^r strain at 37°C for 32 h in CDM with glucose (0.5%), pyruvate (1%), or Casamino Acids (1%) as the primary carbon source (*n* = 3; error bars show pooled standard deviations [SD]).

enzymes necessary for fermentative growth on this substrate. To identify what these targets may be, we first compared the excretion of several key metabolic end products (acetate, formate, lactate, and ethanol) during anaerobic growth of *S. aureus* on either glucose or pyruvate (see Fig. S1 and S2 in the supplemental material). Growth on glucose resulted in a mixture of end product metabolites, a large proportion of which are important for balancing redox stress (L-lactate, D-lactate, formate, and ethanol [EtOH]). *S. aureus* grown anaerobically on pyruvate, on the other hand, generated significantly less lactate and ethanol and significantly more acetate and formate. This result is consistent with high-level flux of pyruvate to acetate for energy production concomitant with a shift from energy-producing glycolysis (2×ATP/glucose consumed) to energy-consuming gluconeogenesis (4×ATP/glucose produced) (Fig. S1).

To confirm that gluconeogenic catabolism of pyruvate proceeds via the predicted ATP-consuming pathway in *S. aureus* (see Fig. S1 in the supplemental material), we measured the growth of wild-type *S. aureus*, Δ*pyc* mutant (*pyc* encodes pyruvate carboxylase), and Δ*pckA* mutant (*pckA* encodes phosphoenolpyruvate carboxykinase) anaerobically on pyruvate (Fig. S2B). Both mutants failed to grow under these conditions. Additionally, we confirmed that acetogenesis (generates 1×ATP/pyruvate [Fig. S1]) was required for anaerobic growth of *S. aureus* on pyruvate, but not on glucose, using an *S. aureus* Δ*ackA* mutant (*ackA* encodes acetate kinase) (Fig. S2C). These data suggest that *S. aureus* requires acetogenesis in order to produce sufficient ATP to maintain

cellular homeostasis and run gluconeogenesis while growing on pyruvate under nonrespiratory conditions.

Partial inhibition of PDHC by NO· limits acetogenesis and growth of *S. aureus* on pyruvate. The requirement for acetogenesis during anaerobic growth on pyruvate suggests that NO· may directly inhibit acetogenic enzymes in *S. aureus* and thus limit growth. Indeed, previous work has shown that PDHC (pyruvate dehydrogenase complex) and Pfl (pyruvate formate lyase), enzymes that catalyze the first committed step in acetogenesis from pyruvate (see Fig. S1 in the supplemental material), are susceptible to NO· inactivation (8). Furthermore, oxygen also inhibits Pfl activity, and thus, PDHC is likely the dominant enzyme for converting pyruvate to acetyl coenzyme A (acetyl-CoA) during our *in vitro* NO· growth assays (14). However, NO· must not completely inactivate PDHC, as acetyl-CoA is an essential precursor metabolite for growth on any carbon source. Thus, we postulated that partial inhibition of PDHC by NO· might be growth limiting for *S. aureus* on pyruvate, but not hexoses, as a result of an increased need for carbon flux through acetyl-CoA to acetate for energy production.

In support of this hypothesis, the *S. aureus* Δ*pflAB* mutant (*pflAB* encodes Pfl) was more susceptible to the PDHC inhibitor triphenylbismuthdichloride (TPBC) when grown anaerobically on pyruvate (MIC = 1.5 μM) than glucose (MIC = 4 μM) (15). Additionally, NO· treatment during growth on pyruvate significantly reduced the intracellular concentration of acetyl-CoA and the "flux" of pyruvate to acetate in wild-type *S. aureus* compared to aerobic and anaerobic growth conditions (Fig. 3A and B). Finally, NO· treatment significantly reduced intracellular ATP levels for *S. aureus* on pyruvate but did not decrease ATP levels for *S. aureus* grown on glucose (Fig. 3C). Given the propensity of bacteria to maintain a constant intracellular level of ATP/cell and the increased demand for acetogenic flux in *S. aureus* grown on pyruvate during nonrespiratory conditions, these data suggest that partial inhibition of PDHC/Pfl by NO· inhibits *S. aureus* growth on pyruvate by limiting ATP production and gluconeogenic flux.

Intracellular *S. aureus* survival requires NO· resistance. During infection, NO· levels within phagosomes of activated phagocytes surpass those known to completely inhibit *S. aureus* respiration (9, 16). Consistent with this, a lactate dehydrogenase-deficient mutant of *S. aureus* (Δ*ldh1*Δ*ldh2*Δ*ddh* mutant) was significantly attenuated for survival in RAW 264.7 macrophages compared to wild-type *S. aureus* (Fig. 4A) (the survival kinetics for wild-type *S. aureus* were the same for *S. aureus* strains COL, Newman, and SF8300 [data not shown]). Furthermore, the survival defect of the Δ*ldh1*Δ*ldh2*Δ*ddh* mutant was completely abrogated by treating the macrophages with the iNOS inhibitor N-iminoethyl-L-lysine (L-NIL). We validated the efficacy of L-NIL treatment by demonstrating reduced levels of extracellular nitrite in macrophages (see Fig. S3A and S3B in the supplemental material). Given that lactic acid fermentation in response to NO· is unique to *S. aureus*, we compared the survival of wild-type *S. aureus* to *Staphylococcus haemolyticus* and *Staphylococcus saprophyticus*. Both CNS exhibited significantly greater susceptibility to macrophage killing than *S. aureus* (Fig. 4B). L-NIL treatment largely reversed these differences, suggesting that *S. aureus* NO· resistance promotes survival during phagocytosis.

S. aureus NO· resistance during phagocytosis is glycolysis dependent. Given our *in vitro* data, we hypothesized that *S. aureus*
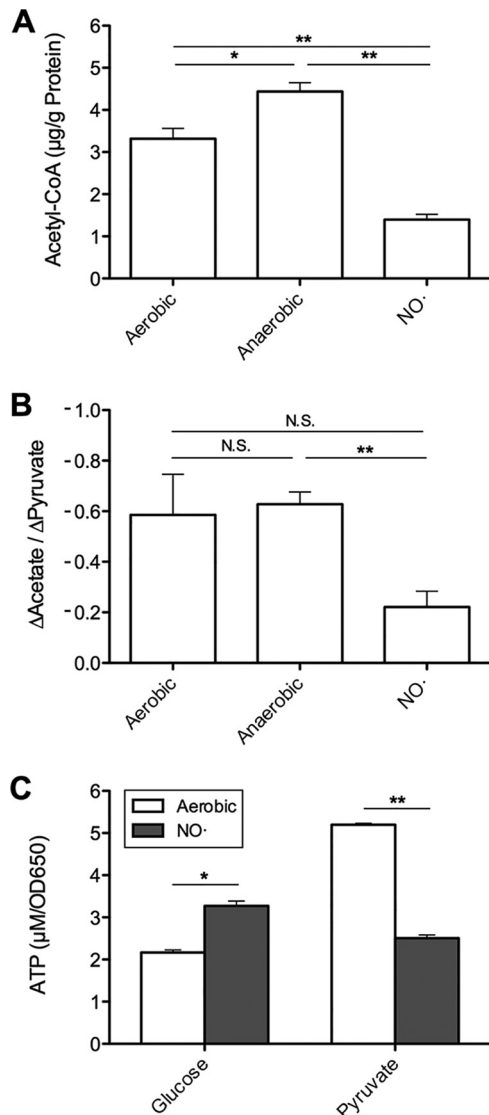
FIG 3 NO· exposure limits acetogenic flux of pyruvate. (A) Average intracellular acetyl-CoA levels for *S. aureus* COL grown at 37°C in CDM with pyruvate (1.1%) as the primary carbon source (*n* = 3; error bars show SEM). (B) Average acetogenic "flux" of pyruvate (acetate produced/pyruvate consumed) for *S. aureus* COL grown at 37°C in CDM with pyruvate (50 mM) as the primary carbon source (*n* = 3; error bars show SEM). (C) Average intracellular ATP levels (in micromolar per OD_{650}) of *S. aureus* COL grown aerobically with or without NO· mix in CDM with glucose (25 mM) or pyruvate (50 mM) as the primary carbon source (*n* = 3; error bars show SEM). Significance was calculated using a Student's two-sided *t* test (*, $P \leq 0.05$; **, $P \leq 0.01$; N.S., not significant).

FIG 4 Lactate fermentation enables *S. aureus* NO· resistance during phagocytosis. (A) Percent survival of wild-type *S. aureus* COL and Δ*ldh1*Δ*ldh2*Δ*ddh* mutant in activated RAW 264.7 macrophages with L-NIL (100 nM) or without L-NIL at 20 h postinoculation (MOI = 10:1) (*n* = 3; error bars show pooled SD). (B) Percent survival of wild-type *S. aureus* COL (SA), *S. haemolyticus* (SH), and *S. saprophyticus* (SS) in activated RAW 264.7 macrophages with or without L-NIL (100 nM) at 20 h postinoculation (MOI = 10:1) ($3 \leq n \leq 4$).The fold effect of L-NIL treatment on bacterial survival is indicated above the bars. Statistical significance was assessed using a Student's two-sided *t* test (**, $P \leq 0.01$; N.S., not significant).

survival during phagocytosis would be glycolysis dependent. To examine this possibility, we constructed *S. aureus* mutants with mutations in several predicted glycolytic genes (*pfkA* [encodes phosphofructokinase], *pyk* [encodes pyruvate kinase], and *gapA* [encodes glyceraldehyde-3-phosphate dehydrogenase A]) and gluconeogenic genes (*pyc*, *pckA*, and *gapB* [encodes glyceraldehyde-3-phosphate dehydrogenase B]) in several strain backgrounds (see Fig. S1 in the supplemental material). To confirm the predicted metabolic roles of these genes, we grew the mutants aerobically in media with either glucose or Casamino
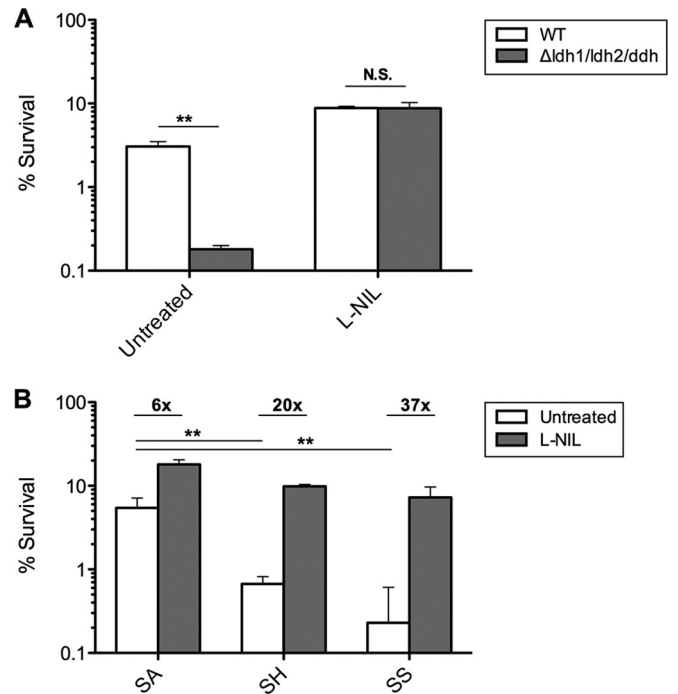
Acids as the primary carbon source. Both *S. aureus* Δ*pfkA* and Δ*pyk* mutants were unable to grow on glucose (i.e., encode glycolytic enzymes), while *S. aureus* Δ*pckA* and Δ*gapB* mutants were unable to grow on Casamino acids (i.e., encode gluconeogenic enzymes) (Fig. S4A and S4B). All other mutants exhibited either no observable phenotype or very small growth defects (Fig. S4C and S4D). These phenotypes were confirmed using two additional *S. aureus* strains (Newman and SF8300 [data not shown]). Complementation restored growth of all *S. aureus* COL mutants on their respective carbon sources (Fig. S3E and S3F).

Next, we examined the survival of the glycolytic (Δ*pfkA* and Δ*pyk*) and gluconeogenic (Δ*pckA* and Δ*gapB*) mutants during phagocytosis by RAW 264.7 macrophages. Both glycolytic mutants (Δ*pfkA* and Δ*pyk* mutants) exhibited significantly reduced survival at 12 and 20 h postinfection (hpi), while the gluconeogenic mutants (Δ*pckA* and Δ*gapB* mutants) displayed no survival defect (Fig. 5A). Attenuation of the glycolytic mutants was not a result of differential bacterial uptake (~75% for all strains) and was completely reversed by L-NIL treatment (Fig. 5B). Furthermore, survival of wild-type *S. aureus* was significantly improved by the addition of increasing amounts of glucose to the tissue culture medium (Fig. 5C). In the absence of NO·, excess glucose had no effect on bacterial survival. Furthermore, glucose treatment did not affect macrophage NO· production (Fig. S3A and S3B). Altogether, these data suggest that *S. aureus* has access to a
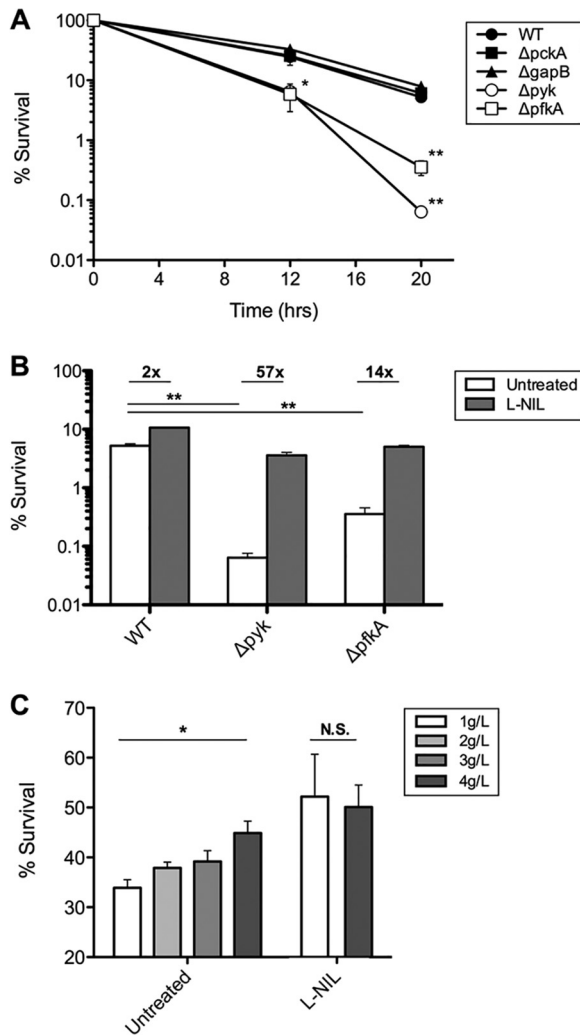
FIG 6 Glycolysis is essential for *S. aureus* virulence during sepsis. C57BL/6 mice were infected via tail vein injection with 7.5×10^6 CFU of wild-type *S. aureus* Newman or $\Delta pckA$ or Δpyk mutant. Kidneys (A) and livers (B) were harvested on 1, 2, and 5 days postinfection, and bacteria were counted ($8 \leq n \leq 12$). Each symbol represents the value for an individual mouse. The lines indicate mean organ burden. The limit of detection was 100 CFU/organ.

FIG 5 *S. aureus* requires glycolysis to resist NO· during phagocytosis. (A) Percent survival of *S. aureus* COL central metabolic mutants in activated RAW 264.7 macrophages at 12 and 20 hpi ($3 \leq n \leq 6$; error bars show pooled SD). (B) Percent survival of *S. aureus* COL glycolytic mutants in activated RAW 264.7 macrophages with or without 100 nM L-NIL at 20 hpi ($5 \leq n \leq 6$; error bars show pooled SD). The fold effect of L-NIL treatment on bacterial survival is indicated above the bars. (C) Percent survival of *S. aureus* COL in activated RAW 264.7 macrophages at 12 h with or without L-NIL treatment in RPMI 1640 with increasing amounts of glucose ($n = 3$; error bars show pooled SD). Statistical significance was calculated using a Student's two-sided t test (*, $P \leq 0.05$; **, $P \leq 0.01$; NS, not significant).

variety of nutrient sources within macrophages, but host NO· necessitates the specific utilization of glycolytic carbon sources as a result of respiration inhibition.

S. aureus virulence in mice is glycolysis dependent. To determine the greater contribution of glycolysis and gluconeogenesis to *S. aureus* pathogenesis, we infected C57BL/6 mice intravenously with wild-type *S. aureus* and *S. aureus* Δpyk, $\Delta pfkA$, and $\Delta pckA$ mutants. Infection with wild-type and gluconeogenic-defective *S. aureus* $\Delta pckA$ mutant produced similar results: both strains colonized and proliferated in the kidney and liver (Fig. 6A and B), and both strains induced ~20% weight loss in infected mice by day 5 (data not shown). Organ burdens and weight loss in the wild type and $\Delta pckA$ mutant were not significantly different. The gly-
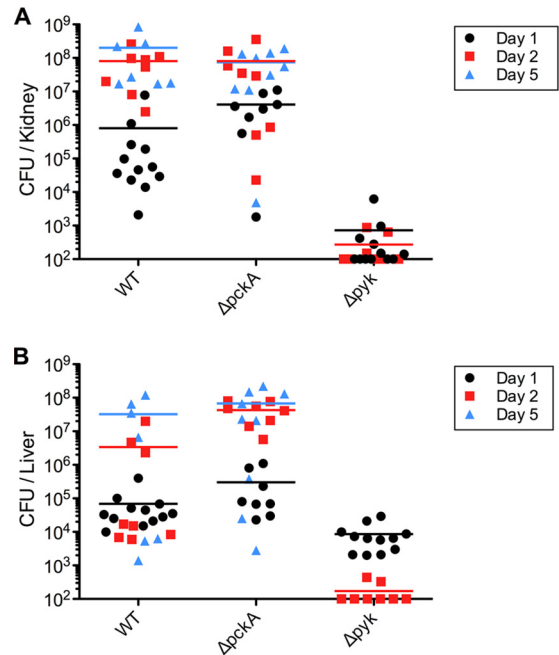
colytic mutants (Δpyk and $\Delta pfkA$ mutants), on the other hand, were significantly attenuated compared to the wild type and were essentially cleared from the kidney and liver by day 2 (Fig. 6A and B and see Fig. S6A and S6B in the supplemental material). Additionally, the *S. aureus* Δpyk mutant exhibited a 6-log-unit decrease in tissue burden (day 7) and an inability to form an open lesion in a skin and soft tissue infection (SSTI) model of *S. aureus* infection (Fig. S5).

To examine the contribution of host NO· production to the observed attenuation of the *S. aureus* glycolytic mutants, we infected both wild-type and iNOS$^{-/-}$ C57BL/6 mice with wild-type *S. aureus* and *S. aureus* Δpyk and $\Delta pfkA$ mutants intravenously. Loss of iNOS resulted in increased burden of wild-type *S. aureus* in the kidney but did not affect the burden of either glycolytic mutant in either organ (see Fig. S6A and S6B in the supplemental material). The failure of iNOS deletion to reverse the attenuation of the glycolytic mutants during sepsis suggests that other selective factors maintain the need for bacterial glycolysis even in the absence of host NO· production. Staining of both uninfected tissue and *S. aureus* tissue abscesses revealed regions of severe tissue hypoxia, suggesting that low oxygen may also necessitate the need for hexose-derived fermentative metabolism independently from NO·-mediated respiration inhibition (Fig. 7 and Fig. S7).

DISCUSSION

Unlike other pathogens, *S. aureus* is capable of growing during high nitrosative stress. *S. aureus* achieves this unique resistance via the induction of an NO·-resistant metabolic state (8). The substrates and central metabolic pathways that support these activi-
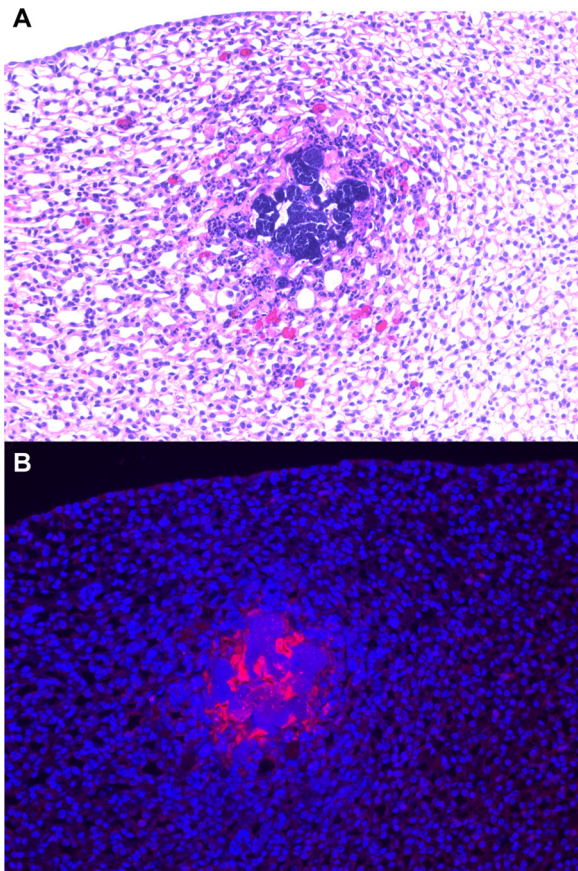
FIG 7 *S. aureus* infected tissues display acute hypoxia. Representative kidney abscesses harvested from C57BL/6 mice on day 2 post-infection with 7.5×10^6 cfu of wild type *S. aureus* Newman were stained with either (A) hematoxylin and eosin (H&E) or (B) Hypoxyprobe (pink) and DAPI (blue). Tissues were imaged at $20\times$ magnification using an Olympus B $\times$ 60 fluorescence microscope.

ties were previously poorly defined. Using a variety of defined medium conditions, we demonstrated that *S. aureus* resistance to high levels of NO· (i.e., levels sufficient to inhibit respiration) is glycolysis dependent both *in vitro* and during phagocytosis. We determined that nonglycolytic carbon sources fail to support NO·-resistant growth due to a combination of respiration-dependent catabolism and partial inhibition of PDHC/Pfl activity. Finally, we showed that glycolysis is required for *S. aureus* pathogenesis in a murine sepsis and SSTI model of infection.

Interestingly, several large *S. aureus* virulence screens have failed to identify glycolysis as an essential component of *S. aureus* virulence (17–19). This can be explained by the fact that the two glycolytic mutants we identified, the Δ*pyk* and Δ*pfkA* mutants, grow very poorly in the glucose-rich media used to generate the transposon libraries (e.g., brain heart infusion [BHI] medium and tryptic soy broth [TSB] [data not shown]). By removing glucose as a substrate for growth and supplying abundant gluconeogenic substrates, we were able to grow *S. aureus* Δ*pfkA* and Δ*pyk* mutants without observable growth phenotypes and identify this metabolic pathway as essential for *S. aureus* pathogenesis. One study previously noted the importance of glycolysis to *S. aureus* virulence, although they utilized an invertebrate model and an *S. aureus* Δ*gapA* mutant (20). We observed no glycolytic defect for

this mutant in three *S. aureus* strains (COL, Newman, and SF8300), implying that GapB is reversible and can compensate for loss of GapA. This discrepancy could be the result of our Δ*gapA* mutants separately acquiring compensatory mutations or the fact that the previously reported mutant was constructed in a highly mutagenized strain of *S. aureus* (NCTC8325-4) (21, 22). Regardless, experimentation with the Δ*pyk* and Δ*pfkA* mutants demonstrates that glycolysis is essential to *S. aureus* virulence.

Glycolysis supports *S. aureus* virulence by promoting growth during innate immune activation. Specifically, a subset of glycolytic carbon sources (hexoses) is compatible with nonrespiratory growth; a selective pressure is generated by host NO· production and abscess formation (i.e., low oxygen). Hexoses support nonrespiratory growth of *S. aureus* because they allow for redox-balanced ATP generation and precursor metabolite formation, while avoiding catabolic pathways that are directly inhibited by NO·. Other metabolic substrates may require quinone-dependent (and thus respiration-dependent) enzymes (e.g., amino acids and lactate), limit carbon availability via excessive fermentation (e.g., mannitol and sorbitol [Fig. S8]), or require NO·-sensitive enzymes for catabolism (e.g., pyruvate). However, hexose catabolism via glycolysis and heterolactic acid fermentation alone cannot fully explain the growth of *S. aureus* during NO· stress, as redox balancing under these conditions requires use of all available glucose for lactic acid production. While EtOH fermentation could alleviate this metabolic stress, and does under anaerobic conditions, we do not observe EtOH production by *S. aureus* following NO· exposure (8). These data suggest that additional, unidentified, redox-balancing reactions support NO·-resistant growth of *S. aureus* on hexoses.

Likewise, nonrespiratory growth induced by low oxygen and host NO· production is probably not the only selective pressure that necessitates *S. aureus* glycolytic metabolism. For instance, iron restriction, as experienced during infection, has been shown to induce expression of *S. aureus* glycolytic and lactic acid fermentation genes and restrict growth of *S. aureus* on gluconeogenic substrates (23, 24). This is a result of the high abundance of iron in respiratory and tricarboxylic acid (TCA) cycle proteins. Despite this, respiratory metabolism has been shown to be important for *S. aureus* virulence, as evidenced by the attenuation of terminal oxidase- and heme-deficient mutants in the hearts and livers of infected mice (25). This discrepancy can likely be explained by the spatiotemporal nature of infection. At certain times, *S. aureus* will have sufficient oxygen and iron to perform respiratory metabolism, but at other times, host iron sequestration, low oxygen, and host NO· production will necessitate glycolytic fermentation. This likely explains the lack of virulence restoration when infecting iNOS$^{-/-}$ mice with the Δ*pyk* and Δ*pfkA* mutants. While host NO· production likely necessitates Pyk and PfkA activity within activated phagocytes (Fig. 5B), the iron-restricted and hypoxic environment of infected tissue also select for high glycolytic flux in *S. aureus*. Thus, the glycolytic requirement for full *S. aureus* virulence is multifaceted, making enzymes in this pathway attractive candidates for antimicrobial development.

Likewise, the concentrations of metabolic substrates available to *S. aureus* may vary according to tissue and stage of infection. A limited supply of gluconeogenic substrates and robust availability of glycolytic substrates during the early stages of infection fits well with our model of *S. aureus* metabolic adaptation to tissue invasion and innate immunity (Fig. 8). For instance, glycolytic sub-
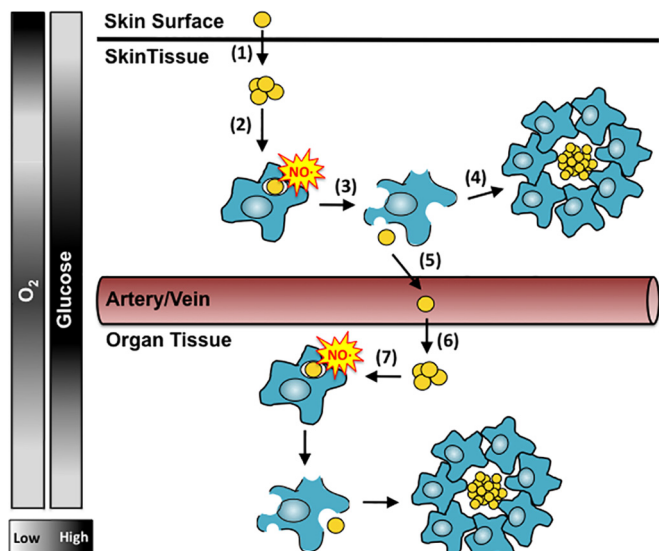
FIG 8 Model: tissue invasion necessitates *S. aureus* glycolytic metabolism. *S. aureus* skin invasion (1) is mediated by virulence factors and/or host tissue damage and is accompanied by decreased oxygen but increased glucose availability. Following tissue seeding, *S. aureus* is phagocytized (2) during which it must employ glycolytic-based fermentation in order to resist the effects of high host NO· production. Toxin expression allows for *S. aureus* escape from the intracellular environment (3). Immune activation results in further influx of cells, which surround *S. aureus* forming an abscess (4) that further limits both oxygen and glucose availability. *S. aureus* able to escape this enclosure disseminate to the blood stream (5), an environment rich in glucose and heme-bound oxygen. From the bloodstream *S. aureus* invades other sterile tissues including the kidney and liver (6). In these organs, a variety of factors necessitate *S. aureus* glycolysis including tissue hypoxia, host NO· production (7), iron limitation, and nutrient availability.

strates are essentially absent in sweat, the primary carbon source for skin-associated staphylococci (26, 27). However, glucose is highly abundant in human serum and certain tissues/organs (e.g., the liver) (28, 29). Furthermore, it is well-known that *Streptococcus*, another Gram-positive extracellular pathogen, relies extensively on carbohydrate metabolism to support growth and virulence (30). Alternatively, intracellular bacteria (e.g., *Listeria*, *Legionella*, *Mycobacterium*, etc.) often rely heavily on gluconeogenic substrates for growth (e.g., fatty acids, glycerol, and amino acids), likely due to the 10:1 nature of gluconeogenic to glycolytic substrates inside the host cell cytoplasm (31–35). While *S. aureus* lacks many of the predicted glycosidases utilized by streptococci for the catabolism of complex carbohydrates (e.g., mucins), the predominantly extracellular nature of *S. aureus* pathogenesis suggests that this bacterium may primarily be using mono- and disaccharides to support growth (the same mono- and disaccharides utilized by host cells to support growth).

Interestingly, people with diabetes (a medical condition characterized by defects in total body glucose homeostasis) are highly susceptible to *S. aureus* infection (36–38). This phenomenon is generally attributed to immune dysfunction among this patient population, as diabetics exhibit increased susceptibility to many pathogens and have documented problems with phagocyte chemotaxis and respiratory burst, despite largely being characterized as hyperinflammatory (39). However, only uncontrolled diabetics (i.e., those exhibiting hyperglycemia) exhibit increased infection rates, suggesting that increased glucose availability may be a key

determinant for *S. aureus* virulence following invasion of sterile tissue (40–42). Furthermore, if these patients are truly hyperinflammatory, then increased glucose availability will promote greater resistance of *S. aureus* to increased host NO· production. This is clear from our observation that *S. aureus* survival during macrophage phagocytosis was improved, in a NO·-dependent manner, when serum glucose levels were increased from normal concentrations (1 g/liter) to the concentrations found in diabetics (2.5 to 4 g/liter). This is especially intriguing given that NO· resistance is a unique feature of *S. aureus* pathogenesis, and infection rates among diabetics are disproportionately increased for *S. aureus* in comparison to other pathogens (38).

These data suggest that the development of bacterium-specific glycolysis inhibitors could be a promising strategy for treating invasive *S. aureus* infections. This is especially important given the increasing drug-resistant nature of many *S. aureus* infections (e.g., methicillin-resistant *S. aureus* [MRSA], vancomycin-resistant *S. aureus* [VRSA], and vancomycin-intermediate *S. aureus* [VISA]). However, glycolysis is a highly conserved metabolic pathway among prokaryotes and eukaryotes, making it especially difficult to selectively target *S. aureus* without inducing detrimental effects in the host. Nonetheless, Zoraghi et al. have identified a novel class of antimicrobials that selectively inhibit *S. aureus* Pyk without inhibiting human Pyk or inducing host cell toxicity (43, 44). They showed that these novel antimicrobial agents were cytotoxic to MRSA, and together we demonstrated that the cytotoxic activity of these compounds was dependent on the presence of Pyk (45). The data presented in this study suggest that this drug could be a powerful antistaphylococcal therapeutic, effective for treating both SSTI and sepsis. Furthermore, several clinically relevant small-colony variants (SCV) of *S. aureus* that are associated with chronic infection presentations are deficient in cellular respiration and thus might be particularly susceptible to a Pyk inhibitor (46).

It is often speculated that the requirement for a given carbon source/central metabolic pathway is simply a reflection of the substrates available to pathogens during growth in their respective infectious niches. However, we have implicated glycolysis as a requirement for *S. aureus* resistance to innate immunity. Given that NO· resistance is a unique feature of *S. aureus* virulence, further investigation into the glycolytic capabilities of the different *Staphylococcus* species is warranted and may in fact reveal a great deal about the disparities that exist in their ability to cause invasive infection.

MATERIALS AND METHODS

Bacterial strains and culture conditions. Staphylococci were cultivated in brain heart infusion (BHI) medium or in chemically defined medium (CDM) in which primary carbon sources could be modified (47). Wild-type (WT) and mutant strains, plasmids, and primers utilized in this study are listed in Table S1 in the supplemental material. Mutants were generated via allelic replacement using the *Escherichia coli*/*S. aureus* shuttle vectors pBT2ts, pBTK, pBTE, and pBTS as previously described (29). Complementation of mutants was carried out by cloning a desired gene under its original promoter into the BamHI site of pOS1 or cloning the gene into the NdeI site of pOS1-*plgt* wherein transcription is driven by the constitutive *lgt* promoter. Aerobic *S. aureus* growth curves were performed at 37°C in 96-well plates (200 μl/well) using a Tecan Infinite M200 Pro microplate reader with 1 mm orbital shaking. Growth was monitored via absorbance at 650 nm (A_{650}) at 15-min intervals. NO· donors were suspended in 0.01 N NaOH and added to cultures at an optical density at 650 nm (OD_{650}) of 0.15 (mid-log phase). The NO· donors utilized in this

study are 2,2′-(hydroxynitrosohydrazono)bis-ethanimine (DETA)/NO (2 and 4 mM) or a mixture of NOC-12 and DEANO (10:1 molar ratio). Anaerobic cultures were grown in tubes (16 by 150 mm) containing 5 ml of medium with stirring at 37°C in a Coy anaerobic chamber.

Growth rate analysis. Growth rate was calculated at 15-min intervals using the following equation: $\Delta \ln A_{650}/\Delta$time (in hours). Aerobic growth rate is the average growth rate during a 2-h window of peak logarithmic growth. NO· growth rate is the average growth rate during a 4-h window from 1 to 5 h after the addition of NO·.

Enzymatic determination of excreted metabolites. Excreted metabolites were harvested from the supernatants of heat-inactivated (70°C for 5 min) culture aliquots. Samples were stored at −20°C and thawed on ice prior to analysis. L-Lactic acid, D-lactic acid, ethanol, formic acid, and acetic acid concentrations were measured enzymatically using commercially available reagents (Roche Yellow Line kits; R-Biopharm AG, Darmstadt, Germany). Pyruvate levels were measured enzymatically (A_{340}) using the following reaction solution: 150 mM Tris-HCl (pH 8.5), NADH (333 μg/ml), and L-lactate dehydrogenase (approximately 14.5 U).

Quantification of intracellular acetyl-CoA levels. *S. aureus* COL cells were grown in 55 ml CDM plus pyruvate (1.1%) in a 125-ml flask at 37°C with shaking at 250 rpm (aerobic and NO·-treated samples). At an OD_{660} of 0.5, DETA/NO (final concentration of 4 mM) was added to one flask, and an equal volume of 10 mM sodium hydroxide was added to the other flask. At 3 min (NaOH flask) and 15 min (DETA/NO flask) after the addition of DETA/NO or NaOH, the *S. aureus* cells were collected via vacuum filtration, washed with 100 ml of 4°C sterile saline, transferred into 600 μl of 4°C sterile phosphate-buffered saline (PBS), and then snap frozen using a dry ice/ethanol bath (total time of ≤5 min). Additionally, *S. aureus* COL cells were grown in 55-ml CDM plus pyruvate (1.1%) in a 125-ml flask in a Coy anaerobic chamber at 37°C with stirring. At an OD_{650} of 0.7, the flask was removed from the anaerobic chamber, and the cells were harvested according to the procedure outlined above for the aerobic and NO·-treated samples. The frozen cells were thawed on ice and then lysed via bead beating. The supernatants were then treated with perchloric acid (final concentration of 0.036 N) and neutralized using potassium bicarbonate (total protein concentrations were measured prior to perchloric acid treatment). We then measured acetyl-CoA concentrations in the samples using the PicoProbe acetyl-CoA assay kit (BioVision Inc.). Acetyl-CoA concentrations were normalized to total protein.

Acetogenic "flux" measurements. The flux of pyruvate to acetate during growth of *S. aureus* was estimated by dividing the amount of extracellular pyruvate consumed by the amount of extracellular acetate produced over a set period of time and measured according to the enzymatic methods described above. For aerobic and anaerobic samples, this period was from the beginning to the end of exponential phase (as determined by a linear growth curve graphed on a log scale). For NO·-treated *S. aureus*, this period was from 1 to 5 h after the addition of NO· (the fermentative window, as determined by sustained lactate production).

ATP measurement. *S. aureus* cells were grown aerobically in the Tecan M200 Pro microplate reader (as described above) in CDM with either glucose (25 mM) or pyruvate (50 mM) as the primary carbon source. At an OD_{650} of 0.15, NO· mix was added to a subset of wells. At 0, 1, 2, 3, 4, and 5 h after the addition of NO·, the intracellular ATP concentrations were determined using the BacTiter-Glo microbial cell viability assay (Promega). ATP levels were then normalized to OD_{650} values for each time point and then averaged over the following time periods: 1 to 3 h after NO· addition for untreated wells (aerobic) and 1 to 5 h after NO· addition in NO·-treated wells.

Phagocytosis assays. RAW 264.7 macrophages were suspended in RPMI 1640 (catalog no. 11875-093; Gibco) supplemented with fetal bovine serum (FBS) (10%) and HEPES (25 mM) at a concentration of 1 × 10⁶ cells/ml, seeded into the wells of a 48-well plate at 0.5 ml/well, and incubated for 18 h at 37°C. The cells were then activated via incubation in RPMI 1640 plus lipopolysaccharide (LPS) (100 ng/ml) and gamma interferon (IFN-γ) (20 ng/ml) for 6 h at 37°C and then spin inoculated in

RPMI 1640 alone with *S. aureus* (opsonized in Hanks balanced salt solution [HBSS] plus 10% mouse serum with active complement at 37°C for 30 min) at a multiplicity of infection (MOI) of 10:1 (*S. aureus* RAW 264.7). Following incubation of the RAW 264.7 cells with *S. aureus* for 30 min at 37°C, the cells were washed twice with PBS and then incubated in RPMI 1640 plus gentamicin (100 μg/ml) for 1 h at 37°C. The infected RAW 264.7 cells were then washed twice with PBS, after which certain wells were treated with 0.01% Triton X-100 to induce RAW 264.7 cell lysis for bacterial enumeration (time zero), while the remaining infected RAW 264.7 cells were incubated in RPMI 1640 plus gentamicin (12 μg/ml) at 37°C for an additional 12 or 20 h. Experiments involving glucose titration utilized RPMI 1640 without glucose (catalog no. 11879-020; Gibco) that was supplemented with FBS (10%), HEPES (25 mM), and tissue culture-grade glucose (1, 2, 3, and 4 g/liter) that was introduced at the time of bacterial inoculation. To inhibit iNOS activity, L-NIL (100 nM) treatment was introduced simultaneously with activation of the RAW 264.7 cells with LPS and IFN-γ and continued for all the following incubations. Nitrite levels of untreated and L-NIL-treated culture supernatants (heat treated at 70°C for 5 min) were measured using the Greiss reaction.

Murine infection models. All mutants utilized for animal infections were first transduced and then confirmed to still exhibit their respective *in vitro* growth phenotypes. For virulence assessment via sepsis, 6- to 8-week-old female WT and iNOS⁻/⁻ C57BL/6 mice from Taconic Farms (Albany, NY, USA) were inoculated via tail vein with 7.5 × 10⁶ CFU of WT *S. aureus* Newman or isogenic mutants in 100 μl of PBS. Weight loss was monitored daily for the period of infection, with mice exhibiting excessive weight loss being sacrificed per the IACUC-approved protocol. At days 1, 2, and 5 postinfection, the kidneys and livers were removed from the infected animals, homogenized in 500 μl sterile PBS, and dilution plated on BHI (WT *S. aureus* Newman and Δ*pckA* mutant) or tryptic soy agar (TSA) without glucose supplemented with 0.5% pyruvate (*S. aureus* Newman Δ*pyk* and Δ*pfkA* mutants) to enumerate CFU. *S. aureus* strain Newman was utilized for these experiments, as weight loss exhibited by mice infected intravenously with this strain correlates reliably with bacterial burdens in the organs, allowing us to monitor disease progression. For virulence assessment in the SSTI model, 6- to 8-week-old female C57BL/6 mice from Jackson Laboratory (Bar Harbor, ME, USA) were injected with 1 × 10⁷ CFU WT *S. aureus* LAC or Δ*pyk* mutant in 20 μl of sterile PBS subcutaneously. The abscess size (length by width) was monitored daily. On day 7, the mice were euthanized, and the abscesses were removed, homogenized in 500 μl of PBS, and dilution plated on TSA without glucose supplemented with 0.5% pyruvate to enumerate CFU. *S. aureus* strain LAC was utilized for the SSTI model, as it belongs to a subtype of *S. aureus* strains (USA300) that are the primary cause of these infections in the United States.

Fluorescence immunohistochemistry. Uninfected C57BL/6 mice and those inoculated with WT *S. aureus* intravenously (i.v.) (7.5 × 10⁶ CFU) 2 days prior were injected intraperitoneally (i.p.) with Hypoxyprobe-1 (Hypoxyprobe Inc., Burlington, MA, USA) (60 mg/kg of body weight) suspended in sterile PBS. After 1 h, liver and kidney tissue was collected, fixed in 10% formalin, paraffin embedded, and sectioned (10 μm) by the Histopathology Core Facility at the University of North Carolina (UNC). Sections were hematoxylin and eosin (H&E) stained by the Histology Core, while unstained sections were prepared for immunohistochemistry as previously described (13). Briefly, unstained sections were deparaffinized using a series of xylene and ethanol washes and then incubated in hot 10 mM sodium citrate buffer (pH 6) for 20 min. Tissues were then blocked in 10% donkey serum (Jackson ImmunoResearch, West Grove, PA) and then stained with affinity-purified anti-Hypoxyprobe-1 rabbit antisera (PAb2627AP; Hypoxyprobe Inc., Burlington, MA, USA) diluted 1:200 in PBS plus 2% donkey serum. Staining was detected using biotinylated secondary antibodies followed by streptavidin-Dylight 594 conjugates (Jackson ImmunoResearch). Stained sections were mounted in ProLong antifade reagent gold with 4′,6′-diamidino-2-phenylindole (DAPI) (Invitrogen, Grand Island, NY, USA)

and viewed with an Olympus BX60 fluorescence microscope. Images were captured using iVision software v.4.0.0 (BioVision Technologies, New Minas, Nova Scotia, Canada).

SUPPLEMENTAL MATERIAL

Supplemental material for this article may be found at http://mbio.asm.org/lookup/suppl/doi:10.1128/mBio.00045-15/-/DCSupplemental.

Figure S1, TIF file, 2.4 MB.
Figure S2, TIF file, 2.7 MB.
Figure S3, TIF file, 2.4 MB.
Figure S4, TIF file, 2.4 MB.
Figure S5, TIF file, 2.4 MB.
Figure S6, TIF file, 2.8 MB.
Figure S7, TIF file, 2.5 MB.
Figure S8, TIF file, 2.6 MB.
Table S1, DOCX file, 0.2 MB.

REFERENCES

1. **Livermore DM**. 2000. Antibiotic resistance in staphylococci. Int J Antimicrob Agents **16:**3–10. http://dx.doi.org/10.1016/S0924-8579(00)00299-5.
2. **Kong HH**. 2011. Skin microbiome: genomics-based insights into the diversity and role of skin microbes. Trends Mol Med **17:**320–328. http://dx.doi.org/10.1016/j.molmed.2011.01.013.
3. **Archer GL**. 1998. Staphylococcus aureus: a well-armed pathogen. Clin Infect Dis **26:**1179–1181. http://dx.doi.org/10.1086/520289.
4. **Xie QW, Cho HJ, Calaycay J, Mumford RA, Swiderek KM, Lee TD, Ding A, Troso T, Nathan C**. 1992. Cloning and characterization of inducible nitric oxide synthase from mouse macrophages. Science **256:**225–228. http://dx.doi.org/10.1126/science.1373522.
5. **Fang FC**. 2004. Antimicrobial reactive oxygen and nitrogen species: concepts and controversies. Nat Rev Microbiol **2:**820–832. http://dx.doi.org/10.1038/nrmicro1004.
6. **Wink DA, Mitchell JB**. 1998. Chemical biology of nitric oxide: insights into regulatory, cytotoxic, and cytoprotective mechanisms of nitric oxide. Free Radic Biol Med **25:**434–456. http://dx.doi.org/10.1016/S0891-5849(98)00092-6.
7. **Clementi E, Brown GC, Feelisch M, Moncada S**. 1998. Persistent inhibition of cell respiration by nitric oxide: crucial role of S-nitrosylation of mitochondrial complex I and protective action of glutathione. Proc Natl Acad Sci U S A **95:**7631–7636. http://dx.doi.org/10.1073/pnas.95.13.7631.
8. **Richardson AR, Libby SJ, Fang FC**. 2008. A nitric oxide-inducible lactate dehydrogenase enables Staphylococcus aureus to resist innate immunity. Science **319:**1672–1676. http://dx.doi.org/10.1126/science.1155207.
9. **Laurent M, Lepoivre M, Tenu JP**. 1996. Kinetic modelling of the nitric oxide gradient generated in vitro by adherent cells expressing inducible nitric oxide synthase. Biochem J **314:**109–113.
10. **Lewis RS, Tamir S, Tannenbaum SR, Deen WM**. 1995. Kinetic analysis of the fate of nitric oxide synthesized by macrophages in vitro. J Biol Chem **270:**29350–29355. http://dx.doi.org/10.1074/jbc.270.49.29350.
11. **Richardson AR, Dunman PM, Fang FC**. 2006. The nitrosative stress response of Staphylococcus aureus is required for resistance to innate immunity. Mol Microbiol **61:**927–939. http://dx.doi.org/10.1111/j.1365-2958.2006.05290.x.
12. **Crooke AK, Fuller JR, Obrist MW, Tomkovich SE, Vitko NP, Richardson AR**. 2013. CcpA-independent glucose regulation of lactate dehydrogenase 1 in Staphylococcus aureus. PLoS One **8:**e54293. http://dx.doi.org/10.1371/journal.pone.0054293.
13. **Thurlow LR, Joshi GS, Clark JR, Spontak JS, Neely CJ, Maile R, Richardson AR**. 2013. Functional modularity of the arginine catabolic mobile element contributes to the success of USA300 methicillin-resistant Staphylococcus aureus. Cell Host Microbe **13:**100–107. http://dx.doi.org/10.1016/j.chom.2012.11.012.
14. **Abbe K, Takahashi S, Yamada T**. 1982. Involvement of oxygen-sensitive pyruvate formate-lyase in mixed-acid fermentation by Streptococcus mutans under strictly anaerobic conditions. J Bacteriol **152:**175–182.
15. **Birkenstock T, Liebeke M, Winstel V, Krismer B, Gekeler C, Niemiec MJ, Bisswanger H, Lalk M, Peschel A**. 2012. Exometabolome analysis identifies pyruvate dehydrogenase as a target for the antibiotic triphenyl-bismuthdichloride in multiresistant bacterial pathogens. J Biol Chem **287:**2887–2895. http://dx.doi.org/10.1074/jbc.M111.288894.
16. **Vodovotz Y, Russell D, Xie QW, Bogdan C, Nathan C**. 1995. Vesicle membrane association of nitric oxide synthase in primary mouse macrophages. J Immunol **154:**2914–2925.
17. **Bae T, Banger AK, Wallace A, Glass EM, Aslund F, Schneewind O, Missiakas DM**. 2004. Staphylococcus aureus virulence genes identified by bursa aurealis mutagenesis and nematode killing. Proc Natl Acad Sci U S A **101:**12312–12317. http://dx.doi.org/10.1073/pnas.0404728101.
18. **Coulter SN, Schwan WR, Ng EY, Langhorne MH, Ritchie HD, Westbrock-Wadman S, Hufnagle WO, Folger KR, Bayer AS, Stover CK**. 1998. Staphylococcus aureus genetic loci impacting growth and survival in multiple infection environments. Mol Microbiol **30:**393–404. http://dx.doi.org/10.1046/j.1365-2958.1998.01075.x.
19. **Mei JM, Nourbakhsh F, Ford CW, Holden DW**. 1997. Identification of Staphylococcus aureus virulence genes in a murine model of bacteraemia using signature-tagged mutagenesis. Mol Microbiol **26:**399–407. http://dx.doi.org/10.1046/j.1365-2958.1997.5911966.x.
20. **Purves J, Cockayne A, Moody PCE, Morrissey JA**. 2010. Comparison of the regulation, metabolic functions, and roles in virulence of the glyceraldehyde-3-phosphate dehydrogenase homologues gapA and gapB in Staphylococcus aureus. Infect Immun **78:**5223–5232. http://dx.doi.org/10.1128/IAI.00762-10.
21. **Novick RP, Richmond MH**. 1965. Nature and interactions of the genetic elements governing penicillinase synthesis in Staphylococcus aureus. J Bacteriol **90:**467–480.
22. **Herbert S, Ziebandt AK, Ohlsen K, Schäfer T, Hecker M, Albrecht D, Novick R, Götz F**. 2010. Repair of global regulators in Staphylococcus aureus 8325 and comparative analysis with other clinical isolates. Infect Immun **78:**2877–2889. http://dx.doi.org/10.1128/IAI.00088-10.
23. **Theodore TS, Schade AL**. 1965. Carbohydrate metabolism of iron-rich and iron-poor Staphylococcus aureus. J Gen Microbiol **40:**385–395. http://dx.doi.org/10.1099/00221287-40-3-385.
24. **Friedman DB, Stauff DL, Pishchany G, Whitwell CW, Torres VJ, Skaar EP**. 2006. Staphylococcus aureus redirects central metabolism to increase iron availability. PLoS Pathog **2:**e87. http://dx.doi.org/10.1371/journal.ppat.0020087.
25. **Hammer ND, Reniere ML, Cassat JE, Zhang Y, Hirsch AO, Indriati Hood M, Skaar EP**. 2013. Two heme-dependent terminal oxidases power Staphylococcus aureus organ-specific colonization of the vertebrate host. mBio **4(4):**e00241-13. http://dx.doi.org/10.1128/mBio.00241-13.
26. **Kutyshenko VP, Molchanov M, Beskaravayny P, Uversky VN, Timchenko MA**. 2011. Analyzing and mapping sweat metabolomics by high-resolution NMR spectroscopy. PLoS One **6:**e28824. http://dx.doi.org/10.1371/journal.pone.0028824.
27. **Harvey CJ, LeBouf RF, Stefaniak AB**. 2010. Formulation and stability of a novel artificial human sweat under conditions of storage and use. Toxicol In Vitro **24:**1790–1796. http://dx.doi.org/10.1016/j.tiv.2010.06.016.
28. **Psychogios N, Hau DD, Peng J, Guo AC, Mandal R, Bouatra S, Sinelnikov I, Krishnamurthy R, Eisner R, Gautam B, Young N, Xia J, Knox C, Dong E, Huang P, Hollander Z, Pedersen TL, Smith SR, Bamforth F, Greiner R, McManus B, Newman JW, Goodfriend T, Wishart DS**. 2011. The human serum metabolome. PLoS One **6:**e16957. http://dx.doi.org/10.1371/journal.pone.0016957.
29. **Fuller JR, Vitko NP, Perkowski EF, Scott E, Khatri D, Spontak JS, Thurlow LR, Richardson AR**. 2011. Identification of a lactate-quinone oxidoreductase in Staphylococcus aureus that is essential for virulence. Front Cell Infect Microbiol **1:**19. http://dx.doi.org/10.3389/fcimb.2011.00019.
30. **Fuchs TM, Eisenreich W, Heesemann J, Goebel W**. 2012. Metabolic adaptation of human pathogenic and related nonpathogenic bacteria to extra- and intracellular habitats. FEMS Microbiol Rev **36:**435–462. http://dx.doi.org/10.1111/j.1574-6976.2011.00301.x.
31. **Myint KT, Uehara T, Aoshima K, Oda Y**. 2009. Polar anionic metabolome analysis by nano-LC/MS with a metal chelating agent. Anal Chem **81:**7766–7772. http://dx.doi.org/10.1021/ac901269h.
32. **McKinney JD, Höner zu Bentrup K, Muñoz-Elías EJ, Miczak A, Chen B, Chan WT, Swenson D, Sacchettini JC, Jacobs WR, Jr, Russell DG**.

2014. Persistence of Mycobacterium tuberculosis in macrophages and mice requires the glyoxylate shunt enzyme isocitrate lyase. Nature **406:** 735–738.

33. **Marrero J, Rhee KY, Schnappinger D, Pethe K, Ehrt S**. 2010. Gluconeogenic carbon flow of tricarboxylic acid cycle intermediates is critical for Mycobacterium tuberculosis to establish and maintain infection. Proc Natl Acad Sci U S A **107:**9819–9824. http://dx.doi.org/10.1073/pnas.1000715107.

34. **Eylert E, Schär J, Mertins S, Stoll R, Bacher A, Goebel W, Eisenreich W**. 2008. Carbon metabolism of Listeria monocytogenes growing inside macrophages. Mol Microbiol **69:**1008–1017. http://dx.doi.org/10.1111/j.1365-2958.2008.06337.x.

35. **Fonseca MV, Swanson MS**. 2014. Nutrient salvaging and metabolism by the intracellular pathogen Legionella pneumophila. Front Cell Microb Biol **4:**12. http://dx.doi.org/10.3389/fcimb.2014.00012.

36. **Lipsky BA, Tabak YP, Johannes RS, Vo L, Hyde L, Weigelt JA**. 2010. Skin and soft tissue infections in hospitalised patients with diabetes: culture isolates and risk factors associated with mortality, length of stay and cost. Diabetologia **53:**914–923. http://dx.doi.org/10.1007/s00125-010-1672-5.

37. **Fowler VG, Jr, Miro JM, Hoen B, Cabell CH, Abrutyn E, Rubinstein E, Corey GR, Spelman D, Bradley SF, Barsic B, Pappas PA, Anstrom KJ, Wray D, Fortes CQ, Anguera I, Athan E, Jones P, van der Meer JTM, Elliott TSJ, Levine DP, Bayer AS, ICE Investigators**. 2005. Staphylococcus aureus endocarditis: a consequence of medical progress. JAMA **293:** 3012–3021. http://dx.doi.org/10.1001/jama.293.24.3012.

38. **Kourany WM, Miro JM, Moreno A, Corey GR, Pappas PA, Abrutyn E, Hoen B, Habib G, Fowler VG, Jr, Sexton DJ, Olaison L, Cabell CH, ICE MD Investigators**. 2006. Influence of diabetes mellitus on the clinical manifestations and prognosis of infective endocarditis: a report from the International Collaboration on Endocarditis-Merged Database. Scand J Infect Dis **38:**613–619. http://dx.doi.org/10.1080/00365540600617017.

39. **Geerlings SE, Hoepelman AI**. 1999. Immune dysfunction in patients with diabetes mellitus (DM). FEMS Immunol Med Microbiol **26:**259–265. http://dx.doi.org/10.1111/j.1574-695X.1999.tb01397.x.

40. **King JT, Goulet JL, Perkal MF, Rosenthal RA**. 2011. Glycemic control and infections in patients with diabetes undergoing noncardiac surgery. Ann Surg **253:**158–165. http://dx.doi.org/10.1097/SLA.0b013e3181f9bb3a.

41. **Kornum JB, Thomsen RW, Riis A, Lervang HH, Schønheyder HC, Sørensen HT**. 2008. Diabetes, glycemic control, and risk of hospitalization with pneumonia: a population-based case-control study. Diabetes Care **31:**1541–1545. http://dx.doi.org/10.2337/dc08-0138.

42. **Dronge AS, Perkal MF, Kancir S, Concato J, Aslan M, Rosenthal RA**. 2006. Long-term glycemic control and postoperative infectious complications. Arch Surg **141:**375–380. http://dx.doi.org/10.1001/archsurg.141.4.375.

43. **Zoraghi R, See RH, Axerio-Cilies P, Kumar NS, Gong H, Moreau A, Hsing M, Kaur S, Swayze RD, Worrall L, Amandoron E, Lian T, Jackson L, Jiang J, Thorson L, Labriere C, Foster L, Brunham RC, McMaster WR, Finlay BB, Strynadka NC, Cherkasov A, Young RN, Reiner NE**. 2011. Identification of pyruvate kinase in methicillin-resistant Staphylococcus aureus as a novel antimicrobial drug target. Antimicrob Agents Chemother **55:**2042–2053. http://dx.doi.org/10.1128/AAC.01250-10.

44. **Zoraghi R, Worrall L, See RH, Strangman W, Popplewell WL, Gong H, Samaai T, Swayze RD, Kaur S, Vuckovic M, Finlay BB, Brunham RC, McMaster WR, Davies-Coleman MT, Strynadka NC, Andersen RJ, Reiner NE**. 2011. Methicillin-resistant Staphylococcus aureus (MRSA) pyruvate kinase as a target for bis-indole alkaloids with antibacterial activities. J Biol Chem **286:**44716–44725. http://dx.doi.org/10.1074/jbc.M111.289033.

45. **Kumar NS, Dullaghan EM, Finlay BB, Gong H, Reiner NE, Selvam JJP, Thorson LM, Campbell S, Vitko N, Richardson AR, Zoraghi R, Young RN**. 2014. Discovery and optimization of a new class of pyruvate kinase inhibitors as potential therapeutics for the treatment of methicillin-resistant Staphylococcus aureus infections. Bioorg Med Chem **22:** 1708–1725. http://dx.doi.org/10.1016/j.bmc.2014.01.020.

46. **McNamara PJ, Proctor RA**. 2000. Staphylococcus aureus small colony variants, electron transport and persistent infections. Int J Antimicrob Agents **14:**117–122. http://dx.doi.org/10.1016/S0924-8579(99)00170-3.

47. **Vitko NP, Richardson AR**. 2005. Laboratory maintenance of methicillin-resistant Staphylococcus aureus (MRSA). John Wiley & Sons, Hoboken, NJ. http://dx.doi.org/10.1002/9780471729259.mc09c02s28.